Eleventh International Conference on CFD in the Minerals and Process Industries
CSIRO, Melbourne, Australia
7-9 December 2015

PREDICTION OF PARTICLE GROWTH DURING MELT SPRAY GRANULATION USING A FIVE-FLUID CFD-PBE APPROACH

Philipp LAU[1] and Matthias KIND[1]*

[1] Karlsruhe Institute of Technology, Department of Thermal Process Engineering, Kaiserstraße 12, 76131 Karlsruhe, GERMANY

*Corresponding author, E-mail address: matthias.kind@kit.edu

ABSTRACT

The process of fluidized bed spray granulation unites the steps of solid formation and product formulation in one apparatus and is used to produce granules out of a liquid. Thereby, a melt is atomized into small droplets and sprayed into the fluidized bed, which consists of seed particles of the same material. Droplets deposit on the particles near the spray zone and form a film which solidifies in the cold fluidization air. Layer-by-layer, granulate products with defined particle sizes are formed.

In a previous investigation, Li et al. (2011) developed a model using computational fluid dynamics (CFD) and population balance equations (PBE) to predict the development of particle size distributions (PSD) in fluidized bed spray systems. Thereby, they focused on low solution spray flow rates (< 5 kg/h per nozzle) and small specific bed masses (< 40 kg/m²).

The aim of this work is to extend this model and to apply it to industrial melt granulation processes with high spray flow rates (> 100 kg/h per nozzle) and high specific bed masses (> 200 kg/m²). Using this CFD-PBE model, it is possible to predict the development of PSD in melt granulation processes using PBE.

For such predictions, it is necessary to evaluate internal process variables, e.g. size-dependent growth rates of the granules, as a function of the current state of the process. This can be obtained using a two-dimensional rotationally symmetric CFD multiphase batch model with one nozzle at its centre. A five-fluid model is solved for short process times (~ s) considering fluid dynamics, particle growth due to drop deposition and energy equations.

Extracting size-dependent and time- and space-averaged particle growth rates, the PBE can finally be solved to predict the particle size distribution for long process times (~ min). The numerical results are validated with experimental data of a melt spray granulation process in batch mode.

NOMENCLATURE

ALR	Air to liquid nozzle ratio, [-].
A_i	Surface of particle phase i, [m²].
α_g	Volume fraction of gas phase, [-].
$\alpha_{p,i}$	Volume fraction of particle phase i, [-].
$d_{droplet}$	Diameter of droplets, [m].
d_{nozzle}	Diameter of nozzle tip, [m]
d_p	Particle diameter, [m].
f_{2mm}	Fluidization number, [-].
G_L	Particle growth rate, [-].
Δh	Height of a grid cell, [-].
K_i	Specific fraction of melt deposited, [1/m²].
$\bar{K}_i$	Time- averaged specific fraction of melt deposited, [1/m²].
L_i	Abscissa of node i, [m].
$\dot{M}_{air,nozzle}$	Mass flow rate of atomizing air, [kg/s].
$\dot{M}_{m,nozzle}$	Mass flow rate of melt, [kg/s].
M_i	Mass of particle phase i, [kg].
$\Delta\dot{M}_{drop}$	Mass flow rate of droplets deposited, [kg/s].
$\dot{M}_{m,in}$	Mass flow of droplets entering cell, [kg/s].
$\dot{M}_{m,i}$	Deposited melt flow on phase i, [kg/s].
$m_{k,i}$	k^{th} moment of distribution i, [m^i].
n_{Gran}	Particle number density, [1/m].
η_i	Deposition efficiency on phase i, [-].
ρ_p	Density of particles, [kg/m³].
q_0	Number distribution, [1/m].
q_3	Volume distribution, [1/m].
t	Time, [s].
$v_{perfPlate}$	Air velocity of perforated plate, [m/s].
$v_{mf,2mm}$	Minimal fluidization velocity of 2 mm particles, [m/s].
v_{drop}	Velocity of droplets, [m/s].
$v_{rel,drop,i}$	Relative velocity between droplets and particle phase i, [m/s].
w_i	Weight of node i, [-].
x_i	Mass fraction of particle phase i, [-].
X_i	Fraction of total droplet deposition on particle phase i, [-].

INTRODUCTION

Tailoring of product properties is becoming increasingly important for the production of solid particles from liquids. Fertilizer, for example, must be easy to dose, free-flowing and dust-free to guarantee a uniform distribution

on the field and trouble-free filling without risk of dust explosion.

Many predominant experimental research contributions on the fluidized bed spray granulation process have been carried out regarding fluid dynamics, interactions between particles and gas (Fan and Zhu, 1998; Geldart, 1986; Jackson, 2000), heat transfer (Schlünder and Tsotsas, 1988), moisture distribution (Heinrich and Mörl, 1999) and growth and agglomeration kinetics (Grünewald, 2011; Peglow et al., 2006; Schaafsma et al., 2000; Zank, 2003). Uhlemann and Mörl (2000) give a good overview of process-relevant mechanisms.

The use and development of numerical simulation tools for design, optimization and scale-up of fluidized bed spray granulation systems is becoming increasingly important due to the fast increase of computer performance. The modelling of multiphase flows in fluidized beds can be divided into the Euler-Euler Model (Two Fluid Model: TFM) and the Discrete Element Method (DEM; Cundall and Strack, 1979).

Using the TFM, which is proposed by Gidaspow (1994), the particle phases are treated as interpenetrating continua. Hereby, the volume fraction of each phase is the characteristic transport quantity. Interactions between particle phases can be modelled using the "kinetic theory of granular flow" (Ding and Gidaspow, 1990; Jenkins and Savage, 1983; Lun et al., 1984). This model has its advantage in modelling a high number of particles, so it can be used to model particulate systems in industrial applications.

According to different applications of granules, a specific product particle size distribution (PSD) is required. Thus, the ability to predict the development of the PSD is crucial for process design, optimization and scale-up. For this reason, population balance equations (PBE) can be solved where the knowledge of so-called internal process variables, e.g. particle size-dependent growth rates, are the important quantities. These internal process variables cannot be obtained by experiments.

Li et al. (2011) developed a model using CFD and PBE to predict the development of PSDs in continuously fluidized bed spray systems with low solution spray flow rates (< 5 kg/h) and small specific bed masses (< 40 kg/m²). Li et al. validated their model with the experimental results of Zank (2003) and Grünewald (2011).

Particle growth rates can be extracted from computational fluid dynamics (CFD) for short process times (~ s), considering a time and spatial resolution of the granulation process. The development of PSD can be predicted for long process times (~ min) by transferring particle growth rates to PBE.

The numerical model in this investigation is extended to industrial-scale melt granulation processes with high spray flow rates (> 100 kg/h) and high specific bed masses (> 200 kg/m²) to predict the development of the product particle size distribution and to optimize such type of processes economically.

MODEL DESCRIPTION AND SET-UP

This investigation focuses on an industrial melt spray granulation process in batch mode (no particles entering and leaving the granulation chamber).

Experimental data can show that certain granulation mechanisms can be neglected. Dust formation is very low in the experiments (no overspray, dust integration or abrasion exists, and the mass of dust in the filter is less than 0.3 % of total product mass of granules) and the number of particles is constant during the process (no internal nucleation, breakage or agglomeration exist). Consequently, only drop deposition is considered here. Therefore, the prediction of the development of PSD can be described with a simple one-dimensional PBE as follows:

$$\frac{\partial n_{Gran}}{\partial t} + \frac{\partial (G_L(d_p) \cdot n_{Gran})}{\partial d_p} = 0 \qquad (1)$$

In order to solve this equation for a given initial condition, it is necessary to know the size-dependent growth rates of the granules G_L as a function of the current state of the process. Hence, a two-dimensional (2D) rotationally symmetric CFD multiphase batch model with one nozzle at its centre is developed. A five-fluid model is solved for short process times (~ s) considering fluid dynamics, particle growth due to drop deposition and energy equations (implemented with user-defined functions).

Extracting size-dependent and time- and space-averaged particle growth rates from CFD, which are not experimentally available, the PBE can be finally solved to predict the particle size distribution for long process times (~ min). The numerical results are validated with experimental data of a melt spray granulation process in batch mode. Figure 1 shows the procedural method for predicting the development of PSD for a melt granulation batch process.

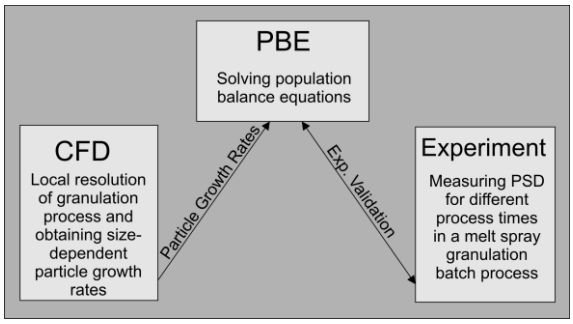

Figure 1: Procedural method for predicting the development of PSD for a melt granulation batch process using CFD and PBE.

CFD Set-Up

The geometry for CFD simulation is based on a cone-shaped single-nozzle fluidized bed spray granulator in batch mode to validate numerical results with experimental data. Assuming that a single-nozzle granulator can be approximated by rotational symmetric flow, a 2D rotationally-symmetric simulation is obtained here. The geometry and the mesh are shown in Figure 2. The mesh is refined in the zone near the nozzle tip by the

use of a grid size function and has 13,062 grid cells and 26,381 nodes. The mesh is adapted twice for the grid independence study. Figure 3 shows that numerical results are independent of the number of grid cells. Therefore, the coarse grid is used for further investigations.

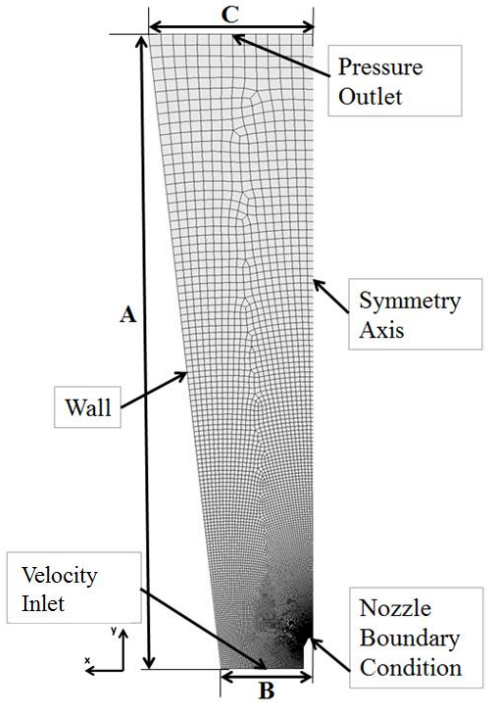

Figure 2: The 2D mesh and boundary conditions of the cone-shaped single-nozzle fluidized bed spray granulation model. The dimensions of the geometry are shown in Table 1.

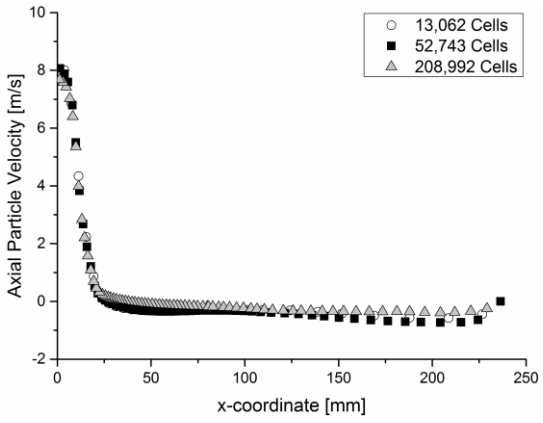

Figure 3: Snapshot axial particle velocity in the cross-sectional area 100 mm above the velocity inlet as a function of distance to the nozzle (x-coordinate) for three different meshes for a process time of 7 s.

The nozzle is realized as a bottom spray configuration and is located in the centre of the granulation chamber. An additional high resolution numerical simulation of the nozzle has been carried out in order to neglect its complex inner structure. A simplified boundary condition for the nozzle could be developed with this high-resolution data. Consequently, it is possible to minimize the grid cells for the complete granulation model. Furthermore, the characteristic droplet diameter of the spray was estimated using phase Doppler anemometry measurements. The results and assumptions of the nozzle are not provided here. Table 1 gives an overview of the geometry and boundary conditions used.

A [mm]	1530
B [mm]	225
C [mm]	400
Geometry	2D-rotationally symmetric
Number of nozzles	1
Boundary conditions	Velocity Inlet (B) Nozzle Wall (A) Pressure Outlet (C) Symmetry Axis
Droplet to nozzle tip ratio	$\frac{d_{droplet}}{d_{nozzle}} = 0.005$
Air to liquid nozzle ratio	$ALR = \frac{\dot{M}_{air,nozzle}}{\dot{M}_{m,nozzle}} = 0.625$
Spray flow rate	$\dot{M}_{m,nozzle} > 100\ {}^{kg}/_{h}$
Fluidization number	$f_{2mm} = \frac{v_{perfPlate}}{v_{mf,2mm}} = 1.8$

Table 1: Details of the geometry and boundary conditions.

Assuming a homogeneous distribution of the fluidization air, the holes in the perforated plate are not considered here. Fluidization and atomization air enter the domain and leave the chamber observed through the pressure outlet boundary condition.

The granulation chamber considered is simulated with CFD using the Euler-Euler multiphase model. It has been shown that this is a possible method to consider a gas/solid flow with a large number of particles (Gidaspow, 1994). In this method, the gas phase and particle phases are treated as penetrated continua. Interactions between different kinds of phases (air, particles and droplets) have to be modelled.

There are different models to characterize the momentum exchange between phases depending on the physical condition of the phases. The interaction between particles and air for fluidized beds can be described with the model of Gidaspow (1994), who combined the models of Ergun (Ergun and Orning, 1952) and Wen and Yu (1966). In the case of the existence of more than one particle phase, the interactions between particles are modelled with the symmetric model of Syamlal and O'Brien (Syamlal, 1987; Syamlal et al., 1993).

The momentum exchange coefficients for granular flows include physical quantities which have to be modelled, e.g. coefficient of restitution and radial distribution functions. Therefore, the so-called "kinetic theory of granular flow" is used. We refer to Gidaspow (1994), Lun and Savage (1984), Syamlal (1987) and Syamlal et al. (1993) for further information. An overview of general

settings and multiphase model quantities used for the CFD simulation are specified in Table 2. These models were also used and validated with experiments by Li et al. (2013).

Euler phases	5 (air, 3 particle phases, melt)
Turbulence model	k-epsilon standard, dispersed
Time step used	0.00001 – 0.0005 s
Solver	Pressure-based, transient
Gravity	-9.81m/s²
Drag "particle-air"	Gidaspow
Drag "particle-particle"	Syamlal and O'Brien
Drag "droplet-air"	Schiller-Naumann
Granular viscosity	Gidaspow
Granular bulk viscosity	Lun et al.
Frictional viscosity	Neglected
Granular temperature	Algebraic
Solids pressure	Lun et al.
Radial distribution	Lun et al.
Packing limit	0.63; constant
Restitution coefficient	0.9; constant

Table 2: Overview of computational multiphase models used for the five-fluid model.

The initial bed mass for the experiment and CFD simulation is 40 kg. The particle size distribution of the seed material was obtained using a Camsizer 2006 (Retsch Technology).

Using the Euler-Euler-model, each particle phase has a defined diameter, so a high number of particle phases are needed to consider a particle size distribution in the process. Due to high numerical costs using a high number of phases, the first six moments of the initial particle size distribution known $q_0(d_p)$ can be reduced to three representative so-called nodes characterized by its weights w_i and abscissas L_i. Therefore, the so-called product difference algorithm is used (Gordon, 1968). Fan and Fox (2008) can show that the use of three representative nodes is sufficient for the description of the fluid dynamics of a particulate system.

The initial bed particle mass of each particle phase can be easily obtained from the ratio of the third moment of considered node *i* to the sum of the third moments of all nodes *j*:

$$\frac{M_i}{\sum_{j=1}^{N} M_j} = \frac{m_{3,i}}{\sum_{j=1}^{N} m_{3,j}} = \frac{w_i \cdot L_i^3}{\sum_{j=1}^{N} w_j \cdot L_j^3} \qquad (2)$$

$m_{0,0}$ [-]	1	M_1 [kg]	1.406
$m_{1,0}$ [mm]	1.6326	M_2 [kg]	20.645
$m_{2,0}$ [mm^2]	2.8693	M_3 [kg]	17.949
$m_{3,0}$ [mm^3]	5.3499	L_1 [mm]	0.944
$m_{4,0}$ [mm^4]	10.4657	L_2 [mm]	1.666
$m_{5,0}$ [mm^5]	21.3052	L_3 [mm]	2.368
		w_1 [-]	0.222
		w_2 [-]	0.596
		w_3 [-]	0.181

Table 3: Details of initial particle size distribution and the reduction to three representative nodes.

Model for drop deposition

Drop deposition is the most important mechanism for particle growth and is implemented with so-called "user-defined functions". The local drop deposition in each computational grid cell is calculated by using the model of Löffler (1988). He describes the local deposition efficiency in two parts, namely the impingement efficiency and the adhesion probability. The impingement efficiency defines the possibility of a droplet hitting the surface of a particle. The adhesion probability defines the probability of a droplet sticking to the particle surface. Both parts depend on the relative velocity between the droplet and particle phase.

The overall deposition efficiency in each cell can be calculated by integrating Löffler's equation. Considering three particle phases and the particle movement (in comparison to a packed bed), the equation is extended by a factor which is the ratio of the relative velocity between drops and particles to the drop velocity. Finally, we obtain equation (3), which is strongly dependent on the relative velocity between particles and droplets.

$$\frac{\Delta \dot{M}_{drop}}{\dot{M}_{m,in}} = 1 - exp\left[-\frac{1.5 \cdot \Delta h}{\alpha_g \cdot v_{drop}} \cdot \sum_{i=1}^{N} \eta_i \frac{\alpha_{p,i} \cdot v_{rel,drop,i}}{d_{p,i}} \right] \qquad (3)$$

The total mass of droplets deposited can be obtained by solving this equation for each grid cell and each particle phase by consideration of conservation, momentum and energy equations. We refer to Bai et al. (2002), Li et al. (2011), Löffler (1988) and Panao and Moreira (2004) for further information.

The numerical simulation is carried out with ANSYS Fluent 15.0.7 on a NEC 128Rc-2 Server on 12 parallel processors (Intel Xeon X5690 6 Core Westmere with 3.46 GHz). The first 20 s are simulated to obtain time-averaged quantities out of CFD.

Experimental Set-up

A single-nozzle batch granulation experiment is used for experimental validation and is shown in Figure 4. The dimensions of the granulation chamber are the same as in Figure 2.

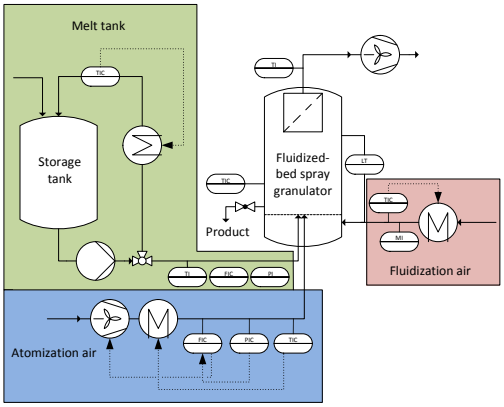

Figure 4: Experimental set-up for validating the numerical granulation model

Particles with a total mass of 40 kg and a defined particle size distribution are filled into the granulation chamber.

The fluidization and atomization air are switched on and the hot melting is recirculated in a storage tank. The valve to the nozzle is opened at the time t = 0 and the melt is atomized into the granulation chamber.

Particles are sampled and analysed with a Camsizer 2006 (Retsch Technology) at 3 min intervals. The fluidized bed is assumed to be ideally mixed due to the high velocities around the nozzle. Taking this into account, the PSD of the sampling is representative for the PSD in the granulation chamber. The loss of the particles sampled is not considered in PBE, because the mass sampled can be neglected due to high bed mass and high melt flow rates. The experiment ends when the pressure drop of the fluidized bed is too high (> 30 mbar). The bed mass increases very quickly due to the high spray flow rate. After 9 min, the first particles are discharged and the experiment is finished.

RESULTS

CFD simulation to extract a particle growth rate

The deposition efficiency is obtained in each cell considering fluid dynamics, drop deposition mechanism and energy equations. With integration over the whole chamber volume, the deposition efficiency of each particle phase i is defined as

$$X_i(t) = \frac{\dot{M}_{m,i}(t)}{\dot{M}_{m,nozzle}} \tag{4}$$

In the case that all melt droplets deposit on particle surfaces, the sum of all X_i equals one:

$$\sum_{i=1}^{N} X_i = X_{tot} = 1 \tag{5}$$

Figure 5 shows the temporal change of X_i for 25 s, considering the first 5 s of the unsteady starting process of the nozzle flow. Considering bubble formation in the fluidized bed due to fluidization and atomization air, the typical fluctuating flow behaviour of the particles is obtained, which influences the current drop deposition rate.

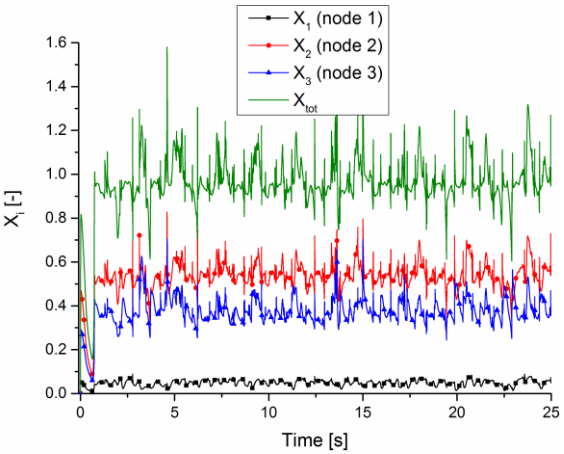

Figure 5: Drop deposition efficiency for each node for the first 25 s of the process.

It can be shown that the highest number of droplets is deposited on node 2, which characterizes the particles with a diameter of 1.66 mm. Due to the high mass fraction of the initial bed of these particle phase, a high surface for drop deposition in the spray zone can be provided.

It can be shown that the time-averaged total deposition efficiency X_{tot} equals one, so the total mass of droplets entering the chamber is deposited on the bed surface. This leads to the conclusion that there is no overspray, due to the high bed height. Experimental results can also show that the effect of overspray can be neglected.

Due to the different surfaces of the nodes used in the simulation, K_i is introduced, which normalizes the proportionate depositing melt flow fraction X_i to the total surface of particle phase i (related to the total particle surface at the beginning, respectively). For short process times (~ s), it can be assumed that the total area of each particle phase is constant.

$$K_i(t) = \frac{X_i(t)}{A_i} \tag{6}$$

With the knowledge of the temporal evolution of K_i, the particle size-dependent growth rate for the first seconds can be obtained using the equation as follows:

$$G_{L,i}(t) = \frac{\partial d_{p,i}}{\partial t} = \frac{2 \cdot K_i(t)}{\rho_p} \cdot \dot{M}_{m,nozzle} \tag{7}$$

The area-specific fraction of deposited droplet mass flow rate K_i is given in Figure 6, neglecting the first 5 s of the unsteady starting process of the nozzle flow.

For a growth rate which depends only on the surface fractions of particle phases, K_i has to be on the same level for each particle phase. Obviously, K_i still seems to be a function of residence time in the spray zone. Larger particles have a higher inertia, so the relative velocity between droplets increases with the increase of particle diameter. Larger particles can collect more droplets during flight, relating to their surface.

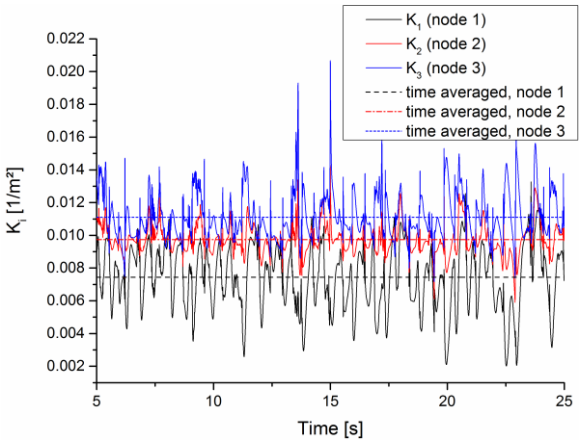

Figure 6: Area-specific fraction of deposited droplet mass flow rate K_i as a function of time.

Due to the unsteady behaviour of the fluid dynamics of particles, K_i has to be averaged in time to obtain a mean drop deposition rate for particle growth rate. Therefore, the evolution of K_i is averaged for 20 s with a linear function. It can be shown that the gradient of this function is near zero, so the time-averaged K_i ($\bar{K}_i$) is the y axis intercept.

Table 4 gives an overview of $\bar{K}_i$ and $G_{L,i}$ which are extracted and calculated from CFD simulation for the first 20 s.

	Node 1	Node 2	Node 3
$\bar{K}_i$ [1/m²]	7.43E-03	9.74E-03	1.11E-02
$G_{L,i}$ [mm/s]	9.276E-04	1.216E-03	1.386E-03

Table 4: Time-averaged K_i which characterizes the drop deposition behaviour in the fluidized bed, which is used to calculate particle size-dependent growth rate $G_{L,i}$.

The particle size-dependent growth rate for the three nodes for the first 20 s (neglecting the first 5 s of unsteady starting process) can be obtained and is given in Figure 7. With a first order approximation, we obtain linear functions for growth rates over particle size.

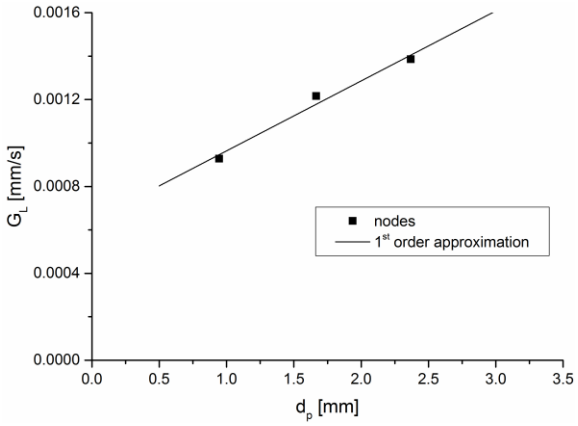

Figure 7: Particle size-dependent growth rate for the first 20 s of the process.

PBE simulation and experimental validation

The development of PSD for long process times (~ min) can be modelled using this growth rate function of short process time (~ s) considering the PBE (see Eq. 1). The PBE is solved with the so-called "high resolution finite volume method", which is a method of second order accuracy. The Van Leer limiter was used for this. We refer to Gunawan et al. (2004) and Leveque (2004) for detailed information. The PBE is solved using MATLAB R2010b.

Due to an unsteady mass flow rate of melt, the particle growth rate changes over time. With the assumption that the fractions of deposited melt droplets are the same, a new growth rate can be extracted by consideration of a new nozzle mass flow rate.

Figure 8 shows the experimental (dots) and numerical (lines) results for the prediction of the development of the particle size distribution over time in the melt spray granulation process considering drop deposition. The experimental results show that larger particles grow faster because of their higher inertia and longer residence time in the spray zone compared to smaller particles. This correlation can also be described by the particle size-dependent growth rate obtained.

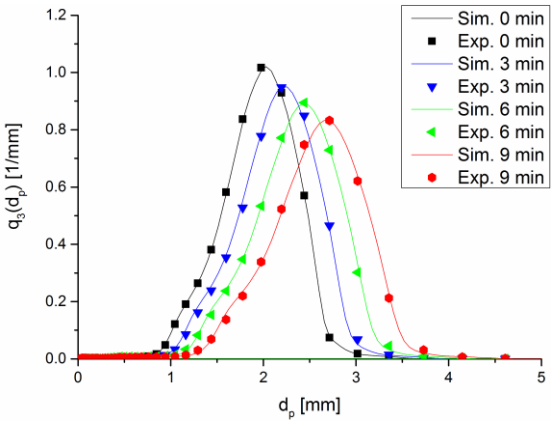

Figure 8: Comparison of numerical (CFD + PBE) and experimental results of the description of the temporal development of PSD.

The numerical model can predict the development of the particle size distribution quite well. Small deviations occur for predicting particles sizes at longer process times (9 s). There are two reasons for the deviations observed. On the one hand, the melt spray flow rates in the experiments vary over time, which is difficult to realize in CFD. On the other hand, the particle size-dependent growth rate is a function of time. The particle size-dependent growth rate for simulating longer process times has to be actualized for better agreement. This actualization has not yet been carried out. Nevertheless, the PSD can be predicted quite well, although the spray flow rates are quite high and the particle growth is fast.

CONCLUSION

The aim of this work is to extend the CFD-PBE model of Li et al. (2011) and to apply it to industrial fluidized bed melt spray granulation processes with high spray flow rates (> 100 kg/h) and high specific bed masses (> 200 kg/m²). Using this model, it is possible to predict the development of the PSD in melt granulation processes and to optimize such type of processes economically.

Therefore, a 2D rotationally symmetric CFD multiphase batch model with one nozzle at its centre was developed. A five-fluid model (air, three particle phases and melt (droplets)) is solved for short process times (~ s) considering fluid dynamics, drop deposition and energy equations (implemented with user-defined functions). Extracting size-dependent and time- and space-averaged particle growth rates from CFD, which are not experimentally available, the population balance was solved to predict the PSD for long process times (~ min).

Comparison of numerical and experimental results shows that this method can predict the particle growth for a specific melt granulation case in batch mode quite well. The CFD model will be validated with other case studies as a future perspective. This model can also be extended to a continuous multi-stage granulation process for longer

process times by updating particle size-dependent growth rates in time.

REFERENCES

BAI, C., RUTSCHE, H. and GOSMAN, A.D., (2002), "Modeling of gasoline spray impingement", *Atomization Sprays*, **12**, 1-27.

CUNDALL, P.A. and STRACK, O.D.L., (1979), "A discrete numerical method for granular assemblies", *Géotechnique*, **49**, 47-65.

DING, J. and GIDASPOW, D., (1990), "A bubbling fluidization model using kinetic theory of granular flow", *AIChE J*., **36**, 523-538.

ERGUN, S. and ORNING, A.A., (1952), "Fluid flow through packed columns", *Chem. Eng. Prog*., **48**, 89-94.

FAN, L.S. and ZHU, C., (1998), "Principles of gas-solid flows", Cambridge University Press.

FAN, R. and FOX, R.O., (2008), "Segregation in polydisperse fluidized beds: Validation of a multi-fluid model", *Chem. Eng. Sci*., **63**, 272-285.

GELDART, D., (1986), "Gas fluidization technology", John Wiley & Sons, Chichester New York Brisbane Toronto Singapore.

GIDASPOW, D., (1994), "Multiphase flow and fluidization: Continuum and kinetic theory description", Academic Press, New York.

GORDON, R.G., (1968), "Error bounds in spectroscopy and nonequilibrium statistical mechanics", *J. Math. Phys.*, **9**, 1087–1092.

GRÜNEWALD, G., (2011), "Staubeinbindung und Keimbildung bei der Wirbelschicht Sprühgranulation", Diss., Cuvillier Verlag.

GUNAWAN, R., FUSMAN, I. and BRAATZ, R.D., (2004), "High resolution algorithms for multidimensional population balance equations", AIChE Journal, 50(11), 2738-2749.

HEINRICH, S. and MÖRL, L., (1999), "Fluidized bed spray granulation – A new model for the description of particle wetting and of temperature and concentration distribution", *Chem. Eng. Process*., **38**, 635-663.

JACKSON, R., (2000), "The dynamics of fluidized particles", Cambridge University Press.

JENKINS, J.T. and SAVAGE, S.B., (1983), "A Theory for the rapid flow of identical, smooth nearly elastic, spherical particles", *J. Fluid Mech*., **130**, 187-202.

LEVEQUE, R.J., (2004), "Finite-volume methods for hyperbolic problems", Cambridge University Press.

LI, Z., (2013), "Fortgeschrittene Methoden zur Beschreibung der Wirbelschicht-Sprühgranulation", Diss., KIT Scientific Publishing.

LI, Z., KIND, M. and GRÜNEWALD, G., (2011), "Modeling the growth kinetics of fluidized bed spray granulation", *Chem. Eng. Technol*., **34**, 1067-1075.

LÖFFLER, F., (1988), "Staubabscheiden", Georg Thieme Verlag, New York.

LUN, C.K.K., SAVAGE, S.B., JEFFREY, D.J. and CHEPURNIY, N., (1984), "Kinetic theories for granular flow: Inelastic particles in Couette flow and slightly inelastic particles in a general flow field", *J. Fluid Mech*., **140**, 223-256.

PANAO, M.R.O. and MOREIRA, A.L.N., (2004) "Experimental study of the flow regimes resulting from the impact of an intermittent gasoline spray", *Exp. Fluids*, **37**, 834-855.

PEGLOW, M., KUMAR, J., WARNECKE, G., HEINRICH, S. and MÖRL, L., (2006), "A new technique to determine rate constants for growth and agglomeration with size- and time-dependent nuclei formation", *Chem. Eng. Sci*., **61**, 282-292.

SCHAAFSMA, S.H., VONK, P. and KOSSEN, N.W.F., (2000), "Fluid bed agglomeration with a narrow droplet size distribution", *Int. J. Pharm.*, **193**, 175–187.

SCHLÜNDER, E.U. and TSOTSAS, E., (1988), "Wärmeübertragung in Festbetten, durchmischten Schüttgütern und Wirbelschichten", Thieme, Stuttgart.

SYAMLAL, M., (1987), "The particle-particle drag term in a multiparticle model of fluidization", National Technical Information Service, Springfield, VA, DOE/MC/21353-2373.

SYAMLAL, M., ROGERS, W. and O'BRIEN, T.J., (1993), "MFIX documentation, theory guide", U.S., Department of Energy, West Virginia.

UHLEMANN, H. and MÖRL, L., (2000), "Wirbelschicht-Sprühgranulation", Springer, Berlin Heidelberg.

WEN, Y. and YU, Y., (1966), "Mechanics of fluidization", *Chem. Eng. Prog. Symp. Series*, **62**, 100-111.

ZANK, J., (2003), "Tropfenabscheidung und Granulatwachstum bei der Wirbelschicht-Sprühgranulation", Diss., Shaker Verlag.

